# Femtosecond dynamics of excitonic absorption in the infrared $In_xGa_{1-x}As$ quantum wells

M. Wegener, I. Bar-Joseph, G. Sucha, M. N. Islam, N. Sauer, T. Y. Chang, and D. S. Chemla
*AT&T Bell Laboratories, Crawfords Corner Road, Holmdel, New Jersey 07733-1988*
(Received 14 November 1988)

We investigate the exciton ionization process in $In_xGa_{1-x}As$ quantum wells using 100-fs time-resolved spectroscopy. The ionization time is studied as a function of temperature. We find a room-temperature ionization time of $\approx 200$ fs and longer times at lower temperatures. At room temperature the ionization is dominated by collisions with LO phonons, whereas at lower temperatures, another extrinsic mechanism becomes increasingly important. We also measure the effect of free electrons and holes versus excitons on the excitonic absorption. We find that excitons are $\sim 3$ times more efficient at room temperature, and that this ratio decreases with temperature. This value is larger than that measured for GaAs. The result is compared with the theory which predicts scaling of the ratio with temperature and the inverse of the exciton binding energy. Good qualitative agreement is obtained.

## I. INTRODUCTION

Semiconductor quantum wells (QW's) have recently attracted much attention because of their electronic transport and optoelectronic properties.[1] The confinement of photocarriers in layers whose thickness $L_z$ is smaller than the bulk material Bohr radius $a_0$ reinforces the excitonic behavior, resulting in an absorption spectrum with clear excitonic resonances that are well resolved even at room temperature.[2–4] Besides its interest for device applications, this unusual feature was found to be important for understanding the origin of both excitonic line shape and optical nonlinearities in QW's.[5] In III-V–compound QW's the binding energy of the quasi-two-dimensional (2D) excitons ($E_b \approx 1-10$ meV) is much smaller than the energy of the polar longitudinal-optical (LO) phonons ($\hbar\Omega_{LO} \approx 30-40$ meV), which interact most strongly with the excitons. Excitons are thus unstable against LO-phonon collisions which can ionize them and release a free electron-hole pair with substantial excess energy. At low temperature the phonon population is scarce and photogenerated excitons are long lived. At high temperature, however, the collision rate increases and the excitonic lifetime can be reduced significantly. Hence the linewidth of QW's excitons consists of two terms: a temperature-independent term related to the QW imperfections and a temperature-dependent one related to the LO-phonon density.[2,3,6] Based on this analysis,[6] experimental investigations of the dynamics of excitonic nonlinearities in GaAs QW's using femtosecond spectroscopic techniques were able to time resolve the room-temperature exciton ionization.[7,8] An unexpected finding of these experiments was that a population of excitons is more efficient than an electron-hole (*e-h*) plasma in reducing the strength of the exciton resonances. This result forced a reexamination of the relative importance of the physical process responsible for excitonic nonlinearities. It was often thought that the dominant mechanism was the unbinding of bound pairs due to screening. The experimental results implied that the underlying Fermi statistics of the exciton's constituents also played an important role through phase-space filling and exchange interaction.[9] In the case of the quasi-2D QW's they show that Debye screening is, in fact, less effective than these two mechanisms. The experimental findings in GaAs QW's were qualitatively explained by a theory[9] that accounts only for the effects of the Fermi statistics and completely neglects the long-range screening. Although the theory explained the general trends of the experiments and gave the right magnitude for exciton and *e-h* plasma nonlinearities within a factor of 2, some quantitative discrepancies remained pertaining to the ratio of these two quantities. Recently, an extension of the theory was proposed by Zimmermann,[10] who used an elegant technique to perform exact infinite summations over all excitonic states (bound and unbound). This extension confirmed the general behavior and provided more accurate values for the nonlinear cross sections. Furthermore, it demonstrated that even in 3D (bulk) semiconductors Pauli exclusion plays a more important role in the nonlinear-optical response of excitons than previously suspected.

Up to now all these experimental investigations were limited to GaAs QW's, because of the availability of efficient femtosecond sources in the visible[11,12] and near infrared.[13] It was not possible to test their generality on other III-V–compound QW systems which have band gaps further in the infrared ($E_g < 1$ eV, i.e., $\lambda > 1.3$ $\mu$m). In this paper we report the first investigation of the dynamics of near-band-edge nonlinearities in high-quality $In_xGa_{1-x}As$ QW's with a 100-fs time resolution. High-quality $In_xGa_{1-x}As/In_xAl_{1-x}As$ and $In_xGa_{1-x}As/InP$ QW structures have been recently developed, because of their wavelength compatibility with light-wave communi-

 

cation technology. This material system presents several interesting features. The excitons in bulk $In_{1-x}Ga_{1-x}As$ have a smaller binding energy ($E_b \approx 2.5$ meV) and larger Bohr radius ($a_0 \approx 300$ Å) than in GaAs. Thus excitons in $In_xGa_{1-x}As$ QW's are closer to the 2D limit and they alloy us to scan a domain of the $k_BT/E_b$ scale that is difficult to reach in GaAs QW's. Furthermore, the QW material is a ternary compound in which alloy disorder can play an important role on exciton line broadening.

In Sec. II we describe our experimental technique with a particular emphasis on the infrared femtosecond source we have used. In Sec. III we present our experimental investigation of the dynamics of exciton saturation at room temperature in a set of $In_xGa_{1-x}As$ QW structures, from which we determine the ionization time of the excitons, $\tau$, and the ratio between the nonlinearities per *e-h* pair and per exciton, $R_{eh/x}$. In Sec. IV we study the temperature dependence of $\tau$ and $R_{eh/x}$. Finally, in Sec. V we compare the results of Secs. III and IV with the present theories.

## II. EXPERIMENTAL TECHNIQUES

There has been significant progress in recent years in tunable subpicosecond laser systems, centered in the visible[11,12] and near-infrared.[13] These systems have been intensively used for spectroscopy of large-band-gap III-V– and II-VI–compound semiconductors. The situation is different concerning short-pulse systems in the range $\lambda > 1$ $\mu$m. Color-center lasers seem to be the only source suitable for short-pulse spectroscopy, covering the spectral window from 1.4 to 1.8 $\mu$m with pulse energies of the order of 10 nJ. Typical pulse width is, however, 4–10 ps. The soliton laser[14] can generate significantly shorter pulses (down to $\approx 20$ fs), but it is of limited value for spectroscopy, primarily because of its complexity and because it is not easily tunable.

An alternative and simpler source of subpicosecond pulses in this frequency range can be constructed by taking advantage of the special way in which optical pulses propagate in a fiber in the negative group-velocity–dispersion region. It was recently reported[15,16] that 100-ps pulses from a neodymium-doped yttrium aluminum garnet (Nd:YAG) laser operating at 1.32 $\mu$m that are launched into an optical fiber emerge from it compressed to 100-fs pulses. It was also reported that the spectral content of these pulses is a broad continuum, extending over about 100 nm. The mechanism responsible for this process has been throughly investigated recently.[17] It can be summarized as follows: In the anomalous group-velocity–dispersion region, small modulations on the input laser are amplified by modulation instability. This causes the input pulse to break up into a series of short pulses which are very nearly solitons. The Raman gain, which in the time domain can be viewed as the soliton self-frequency shift, causes these pulses to propagate at different velocities up to a point where they collide inelastically to form an intense ultrashort pulse.

Based on this concept we have developed a new system, consisting of a Nd:YAG-pumped NaCl color-center laser and an optical fiber.[17] This short-pulse system is very well suited to the study of $In_xGa_{1-x}As$ quantum wells because of its broad spectral output. We start with (10–15)-ps pulses at a repetition rate of 100 MHz from the color-center laser operating at 1.5 $\mu$m, and we couple an average power of 80–100 mW into a dispersion-shifted fiber ($\lambda_0 = 1.41$ $\mu$m). The time autocorrelation of the fiber output yields a pulse width of $\approx 100$ fs full width at half maximum (FWHM) of the pulses, whereas the spectrum is a broad continuum, approximately flat from 1.55 to 1.8 $\mu$m. This spectral width is much larger than that corresponding to a bandwidth-limited 100-fs pulse ($\approx 30$ nm). These and other measurements[17] indicate that the output of the fiber changes from one pulse of the NaCl laser to the next. It consists of a fundamental soliton that is centered around different wavelength from pulse to pulse. The observed broad spectrum is therefore a statistical ensemble of pulses. Measurements of the cross correlation between different parts of the spectrum, selected with interference filters, show that the cross correlation drops by a factor of 20 when we mix 1.6 and 1.7 $\mu$m. However, this drop is about 50% when we mix wavelengths that are 50 nm apart and less than 20% if they are separated by 25 nm.[17] For the time-resolved experiments interference filters with a (30–50)-nm bandwidth are used to select the pump pulse from this broad spectrum. Figure 1 shows the time autocorrelation after such an interference filter. It is seen that the pulses are not broadened, and that the actual pulse width after the interference filters is $\approx 120$ fs. The obtained autocorrelation FWHM is the same (within 20 fs) for all the filters used. A close inspection of the autocorrelation signal reveals that it is not zero at very early or late times ($> 1$ ps), but there is a small background, of the order of 1%, that extends over $\approx 10$ ps. This pedestal is generated by the uncompressed part of the NaCl color-center–laser pulse and comes later than the femtosecond pulse.[17] It dominates at wavelengths close to the color-center wavelength and it decreases at longer wavelengths. The energy content of the pedestal at the wavelengths above 1.55 $\mu$m is about $\frac{1}{3}$ of the total energy.

The time-resolved experiments on $In_xGa_{1-x}As$ QW's

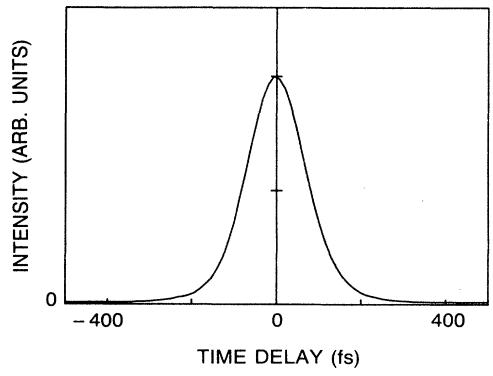


FIG. 1. Autocorrelation of the fiber output after an interference filter centered around 1635 nm. The width of the autocorrelation corresponds to a FWHM of 120 fs for the pulse.

were performed using a conventional pump-probe configuration, where the normalized differential change in the probe intensity transmitted through the QW sample, $\Delta T/T$, is measured by the lock-in technique. Because of the fast fluctuations in the intensity of the pump and the probe at given wavelength, only effects that are linear in the intensity (i.e., far from any saturation regime) can be studied. All experiments were performed in such a small signal regime with $\Delta T/T \approx 2\%$, in which case $\Delta T/T \approx (\Delta\alpha)l$. We verified experimentally that the signal $\Delta T/T$ is proportional to the pump intensity over more than 1 order of magnitude. We have typically used 5 pJ pump-pulse energy corresponding to a peak power of $\approx 50$ W. The pump beam was focused to a 100-$\mu$m-diam spot, such that the energy density is about 50 nJ cm$^{-2}$, thus generating a carrier density $\approx 3\times 10^9$ cm$^{-2}$. The ratio of the pump energy to the probe energy is kept larger than 100. To properly eliminate the effect of the long pedestal, we measured the differential spectrum for $t \approx -1$ ps and subtracted it from the data taken around $t \approx 0$. By decreasing the input power into the fiber it is almost possible to eliminate the pedestal, at the expense of a worse signal-to-noise ratio, without any observed changes of the $\Delta T/T$ behavior on a femtosecond time scale.

The transmitted probe is detected through a 0.22-m spectrometer with a PbS detector. Differential signals as low as $\Delta T/T = 10^{-4}$ could be measured. Typical levels were in the $(1-3)\times 10^{-2}$ range.

Since the expected relaxation times are of the order of the pulse duration, special care is taken to eliminate the contribution of four-photon mixing, known as the "coherent artifact." This is done by cross polarizing the pump and the probe. We have verified experimentally that most of the coherent coupling is eliminated in this configuration by measuring the signal both for parallel and crossed polarization. The signals obtained are of similar magnitude; furthermore, we found that the difference between the parallel and the crossed polarization reproduces the profile of the pulse electric field coherence function[18] of Fig. 1. These experiments were performed at several wavelengths at the exciton resonance and above resonance and give the same results.

## III. EXCITON AND PLASMA NONLINEARITIES IN $In_xGa_{1-x}As$ QUANTUM WELLS

The samples which we studied were $In_xGa_{1-x}As$ multiple quantum wells (MQW's) with either $In_xAl_{1-x}As$ or InP barriers. The first type was grown by molecular-beam epitaxy (MBE) and the other by gas-source MBE. Four different samples were investigated: three were $In_xGa_{1-x}As/In_xAl_{1-x}As$ MQW samples with well widths of 200 Å (60 periods), 150 Å (100 periods), and 100 Å (100 periods) all with 100-Å barriers, and one was an $In_xGa_{1-x}As/InP$ MQW sample with 100-Å well and barrier widths (100 periods). Figures 2 and 3 show the low-temperature (10 K) and room-temperature absorption spectra of two samples: the $L_z = 200$ and the 100 Å $In_xGa_{1-x}As/In_xAl_{1-x}As$ MQW's. The $L_z = 100$ Å sample displays clear heavy-hole (hh) and light-hole (lh) exciton resonances, whereas in the $L_z = 200$ Å sample these two excitons have merged into a single resonance because energy separation between $n_z = 1$ hh and lh is only 6 meV for such a well width. The spectra around the $n_z = 1$ resonances have been fitted to semiempirical line shapes consisting of Gaussian resonances and a broadened 2D continuum with Sommerfeld enhancement[6] to determine the exciton binding energies and linewidths. The binding energies are found to be rather small, $E_b \approx 4$ meV. The measured exciton half-width at half maximum, $\Gamma$, is shown as a function of temperature in Figs. 4(a) and 4(b) for the two samples. The data are well defined by a sum of a temperature-independent term $\Gamma_0$ and a temperature-dependent term $\Gamma_{\rm hom}$,[5,6]

$$\Gamma = \Gamma_0 + \Gamma_{\rm hom}(T) , \tag{1}$$

with

$$\Gamma_{\rm hom}(T) = \frac{\Gamma_1}{\exp(\hbar\Omega_{\rm LO}/k_B T) - 1} . \tag{2}$$

In the ternary alloy $In_xGa_{1-x}As$ two phonon modes are present: a "GaAs-like" mode ($\hbar\Omega_{\rm LO} = 33.4$ meV) and an "InAs" mode ($\hbar\Omega_{\rm LO} = 28.0$ meV).[19] They have very close

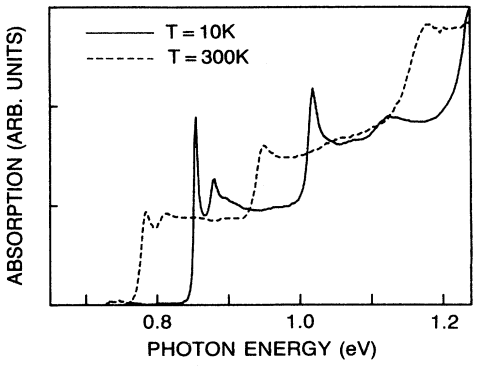


FIG. 2. Absorption spectra of the 100-Å $In_xGa_{1-x}As/In_xAl_{1-x}As$ MQW at 10 and 300 K, respectively.

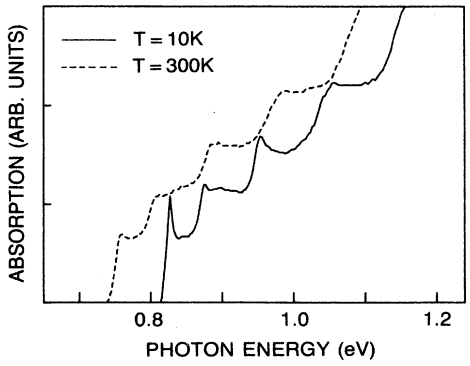


FIG. 3. Absorption spectra of the 200-Å $In_xGa_{1-x}As/In_xAl_{1-x}As$ MQW at 10 and 300 K, respectively.

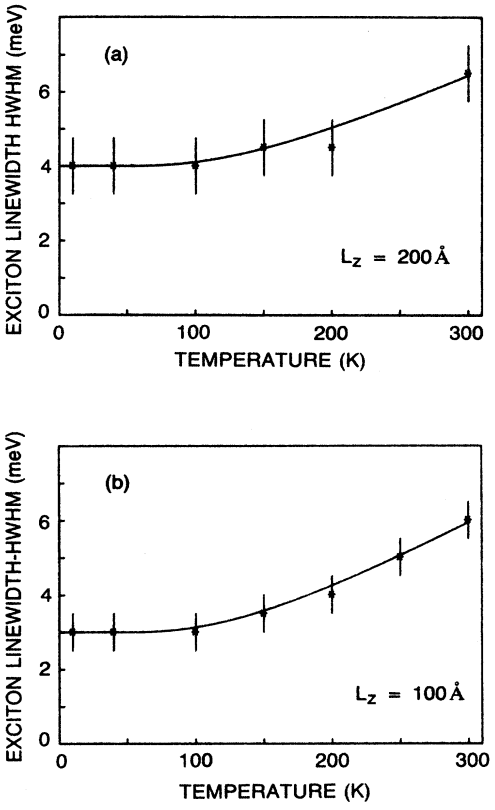


FIG. 4. Linewidth [half-width at half maximum (HWHM)] of the excitonic resonance as a function of temperature for (a) the 200-Å $In_xGa_{1-x}As/In_xAl_{1-x}As$ MQW and (b) the 100-Å $In_xGa_{1-x}As/In_xAl_{1-x}As$ MQW.

energies and, hence, we can describe them by a single effective phonon with an energy $\hbar\Omega_{LO}=35$ meV. We obtain for the $L_z=100$ Å sample $\Gamma_0=3$ meV and $\Gamma_1=9$ meV, and for the $L_z=200$ Å sample $\Gamma_0=4$ meV and $\Gamma_1=7$ meV.

The recombination time in these two samples is longer than the 10-ns separation between successive laser pulses. In order to shorten this lifetime to a few nanoseconds, helium ions were implanted in the 100-Å $In_xGa_{1-x}As/In_xAl_{1-x}As$ sample and protons were implanted in the 200-Å $In_xGa_{1-x}As/In_xAl_{1-x}As$ sample, creating a density of damage sites of $10^{12}$ cm$^{-2}$. We have measured the recombination time to be $\approx 1$ ns. Thus we have a complete recovery of the sample absorption from one laser pulse to the other. The absorption spectra measured at room temperature before and after the implantation show no observable change. The spectral region of the $n_z=1$ resonance and two different pump spectra for resonant and above-resonant excitation are shown in Fig. 5. We first consider the case of resonant excitation of the exciton. In order to get information about the induced changes of the exciton absorption, we detect the change in the transmitted intensity of the probe at the center of the excitonic resonance. This position is determined by the fit to the linear absorption spectrum. It is only slightly displaced from the position of the maximum of the absorption spectrum. It was verified that identical results are obtained when the time response is integrated over a spectral window that covers the excitonic resonance. The time dependence of $\Delta T/T$ is shown in Fig. 6. It exhibits an overshoot that is clearly asymmetric in time. The rise-time corresponds to the pulse duration and the falltime is longer. The differential absorption then reaches a steady state which is constant for a few hundred picoseconds. Our interpretation of these results follows closely that developed for GaAs QW's.[7,9] The resonant pump pulse generates excitons that inhibit further creation of excitons because of phase-space filling and exchange interaction. Shortly thereafter (100–200 fs) the excitons are ionized and dissociate into free *e-h* pairs. At this temperature the plasma is less effective in reducing the excitonic absorption than the exciton gas,[9] and its effect persists until the electrons and holes recombine. To analyze the experimental data quantitatively, we translate this se-

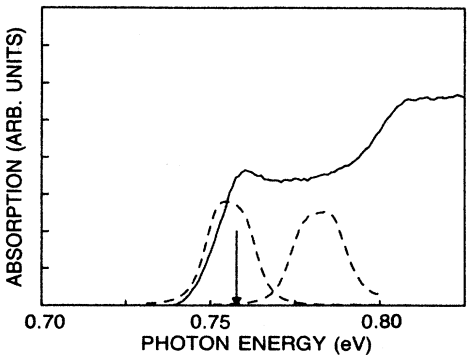


FIG. 5. Detail of the room-temperature absorption spectrum of the 200-Å $In_xGa_{1-x}As/In_xAl_{1-x}As$ MQW around the $n_z=1$ resonance, together with the two pump spectra for resonant and above-resonant excitation. The probe wavelength is indicated by the arrow.

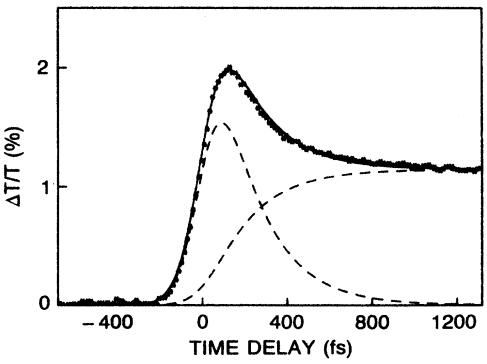


FIG. 6. Time scan of the differential transmission of the 200-Å $In_xGa_{1-x}As/In_xAl_{1-x}As$ MQW at $T=300$ K under resonant excitation (see Fig. 5), $\hbar\Omega_{test}=0.758$ eV. The fit is described in the text. The two dashed lines show the two contributions of excitons and *e-h* pairs, respectively, separated.

quence of events in the following model. Since we are in the small signal regime we can assume that the change in exciton oscillator strength is linear in the density of exciton, $N_x$, or *e-h* pairs, $N_{eh}$, and write[9]

$$\frac{\Delta f}{f} \propto -\left[\frac{N_x}{N_s^x}+\frac{N_{eh}}{N_s^{eh}}\right] \propto -(R_{eh/x}N_x+N_{eh}) , \quad (3)$$

where $N_s^x$ and $N_s^{eh}$ are the corresponding exciton and *e-h* plasma saturation densities and $R_{eh/x}=N_s^{eh}/N_s^x$ is their ratio. In the interval $-0.5<t<+1.5$ ps the recombination and other slow processes that change the densities can be neglected, so that the evolution of the two populations is governed by the rate equations

$$\frac{dN_x}{dt}=P_x(t)-\frac{N_x}{\tau} , \quad (4a)$$

$$\frac{dN_{eh}}{dt}=P_{eh}(t)+\frac{N_x}{\tau} , \quad (4b)$$

where $\tau$ is the exciton ionization time, and $P_x(t)$ and $P_{eh}(t)$ are the generation rates for excitons or *e-h* pairs, respectively. The time dependence of $P_x(t)$ and $P_{eh}(t)$ is taken to be that of a $\mathrm{sech}^2$ pulse with the same width as the autocorrelation of the pump pulse shown in Fig. 1. The time evolution of $\Delta T/T$ depends only on the two physically relevant parameters: $R_{eh/x}$ and $\tau$. The ideal situation of perfect resonant pumping of the exciton resonance corresponds to $P_{eh}(t)=0$. Using Eqs. (3) and (4) we obtain a unique and excellent fit to the data also shown in Fig. 6. The best-fit parameters are $R_{eh/x}=2.7$ and $\tau=200\pm30$ fs. If the exciton ionization is governed by LO-phonon collision, we should have

$$\tau \approx 1/\Gamma_{\mathrm{hom}} . \quad (5)$$

We find that this is indeed the case at $T=300$ K, since $1/\Gamma_{\mathrm{hom}}(300\ \mathrm{K})=260\pm50$ fs. We note, however, that strictly speaking, direct generation of some *e-h* pairs ($P_{eh}\neq0$) is unavoidable because the absorption tail of the continuum extends below the exciton absorption. In order to evaluate the influence of some direct generation of free *e-h* pairs on the parameters, we have repeated the fit assuming a pessimistic upper limit of $P_{eh}=0.5P_x$. In this case we obtain a good fit with $R_{eh/x}=3.5$ and the same value, $\tau=200\pm30$ fs, for the ionization time. We can thus safely conclude $R_{eh/x}=3\pm0.5$.

In the limit $k_BT/E_b \gg 1$ the theory of Schmitt-Rink *et al.*[9] predicts, for $R_{eh/x}$, an asymptotic linear dependence,

$$R_{eh/x}=0.36(k_BT/E_b) . \quad (6)$$

From the line-shape analysis of the linear absorption spectrum, we find $E_b \approx 4$ meV for this sample, giving a theoretical value $R_{eh/x}=2.25$, comparable with our experimental finding. More importantly, the theory predicts the correct dependence of $R_{eh/x}$ as a function of $E_b$ when comparing QW materials with such widely different band gaps as $In_xGa_{1-x}As$ and GaAs. This translates the reduced overlap between the *e-h* states occupied by a warm plasma and those of which the exciton wave function is built. It is, however, interesting to note that this theory gives values of $R_{eh/x}$ which are somehow smaller than the experimental ones both for $In_xGa_{1-x}As$, $R_{eh/x}\simeq2.7$, and for GaAs, $R_{eh/x}\simeq2$. This point will be discussed in more detail in Sec. V. In order to further test the model, we have investigated the case $P_x(t)\approx0$ by pumping above the exciton using a pump with the high-energy spectrum shown in Fig. 5. Figure 7 shows the time evolution of $\Delta T/T$ in this case. The absolute magnitude of the data is not corrected for the drop of the cross-correlation for this detuning. As expected, the overshoot is significantly reduced as compared to resonant pumping. The residual overshoot can be explained by the low-energy tail of the pump spectrum which extends into the exciton line, thus generating some excitons.

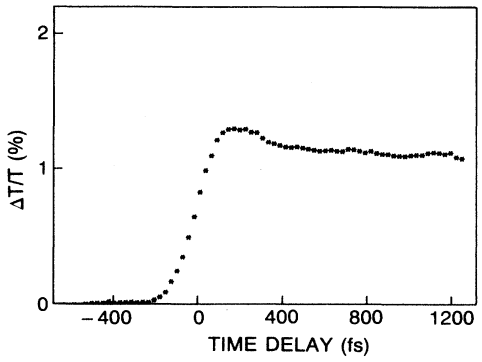


FIG. 7. Time scan of the differential transmission of the 200-Å $In_xGa_{1-x}As/In_xAl_{1-x}As$ MQW at $T=300$ K under above resonant excitation (see Fig. 5), $\hbar\Omega_{\mathrm{test}}=0.758$ eV.

## IV. TEMPERATURE DEPENDENCE OF THE EXCITON DYNAMICS

The ionization by LO-phonon collision is a sensitive function of temperature through the phonon density. Similarly, the occupation by the *e-h* plasma of states which form the exciton wave function is a very sensitive function of $k_BT/E_b$. Hence, temperature is expected to strongly influence both $\tau$ and $R_{eh/x}$, providing a good test of the models. Because of the limited tuning range of our femtosecond pulse source, we could only explore temperatures between $T=300$ and 150 K. Figures 8 and 9 present the dynamics of $\Delta T/T$ at $T=$ 200 and 150 K. Again, they are easily fitted with our simple model, as shown by the solid and dashed lines. Table I summarizes

TABLE I. Comparison of experimental data and theoretical results for the *e-h* and/or exciton nonlinearities in $In_xGa_{1-x}As$ quantum wells. Experimental ionization time compared to the inverse of the temperature-dependent broadening.

| $T$ (K) | $\tau_{\mathrm{expt}}$ (fs) | $\tau_{\mathrm{theor}}$ (fs) | $R_{eh/x}^{\mathrm{expt}}$ | $R_{eh/x}^{\mathrm{theor}}$ |
|---|---|---|---|---|
| 300 | 200 | 260 | 2.7 | 2.3 |
| 200 | 300 | 620 | 2.4 | 1.5 |
| 150 | 350 | 1330 | 1.8 | 1.2 |

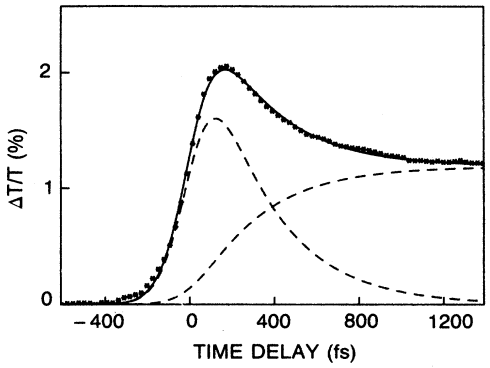


FIG. 8. Time scan of the differential transmission of the 200-Å $In_xGa_{1-x}As/In_xAl_{1-x}As$ MQW at $T=200$ K, $\hbar\Omega_{test}=0.787$ eV.

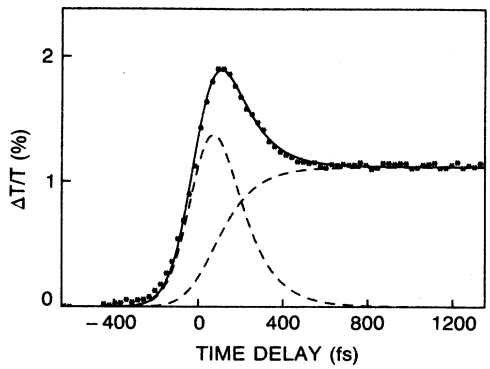


FIG. 10. Time scan of the differential transmission of the 100-Å $In_xGa_{1-x}As/In_xAl_{1-x}As$ MQW at $T=300$ K, $\hbar\Omega_{test}=0.784$ eV.

the values of $R_{eh/x}$ and $\tau$ deduced from the fit assumming $P_{eh}=0$ and compares them to those obtained by Eqs. (5) and (6). The decrease of $R_{eh/x}$ with temperature predicted by the theory[9] is confirmed. Again, this is easily interpreted in terms of the influence of the underlying Fermi statistics, because at low temperature the *e-h* plasma more efficiently populates the states close to the bottom of the bands that are used to build the exciton wave function.

The reduced phonon population at low temperature should give rise to a longer ionization time. The values of $\tau$ given in Table I indeed confirm this general trend, but they are significantly smaller than the values of $1/\Gamma_{hom}$ deduced from the temperature-dependent broadening. This discrepancy indicates that there exists yet another ionization process, which does not depend strongly on the temperature in the range we have explored. In this case the low-temperature exciton linewidth should be expressed as

$$\Gamma_0=\Gamma_{int}+\Gamma_{extr} . \quad (7)$$

In Eq. (6), $\Gamma_{inh}$ is a "static" inhomogeneous broadening due to alloy disorder and well-width fluctuations that does not contribute to the exciton ionization, whereas $\Gamma_{extr}$ is the homogeneous broadening associated with the extrinsic ionization mechanism. One possible candidate for such a mechanism is the ionization of excitons by random electric fields generated by ionized impurities. With this assumption we obtain $\Gamma_{extr}\approx 1$ meV, corresponding to an ionization time of 600 fs. According to this interpretation the ionization of excitons at 300 K is mainly intrinsic, i.e., dominated by collisions with LO phonons, whereas at decreasing temperature the extrinsic ionization mechanism becomes more important as the temperature decreases. The significance of extrinsic effects is further confirmed by studying three other samples as shown in Fig. 10 for a 100-Å $In_xGa_{1-x}As/In_xAl_{1-x}As$ MQW. Table II summarizes the room-temperature values of $R_{eh/x}$ and $\tau$ for the four samples, showing clustering of $R_{eh/x}$ around 3, but larger variations of $\tau$ from sample to sample between 100 and 200 fs.

Let us note that a related pump-probe experiment has been performed in $In_xGa_{1-x}As/InP$ QW's at $T=5$ K with a time resolution of several picoseconds. However,

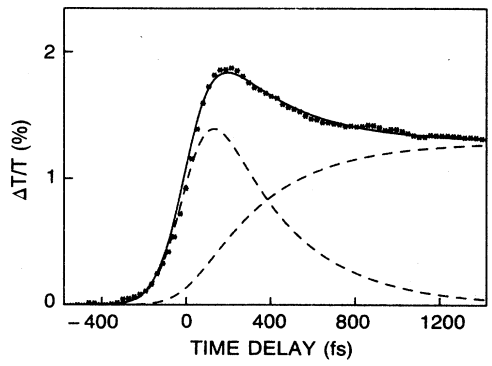


FIG. 9. Time scan of the differential transmission of the 200-Å $In_xGa_{1-x}As/In_xAl_{1-x}As$ MQW at $T=150$ K, $\hbar\Omega_{test}=0.802$ eV.

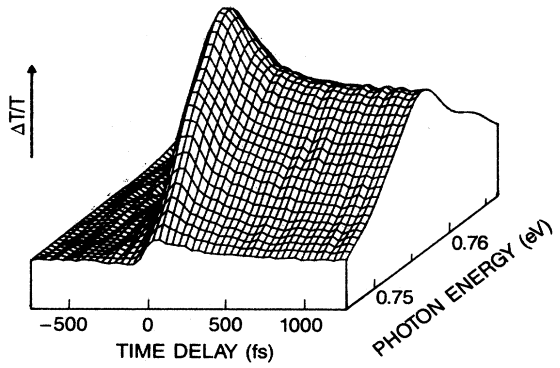


FIG. 11. Spectral and temporal dependence of the differential transmission of the 200-Å $In_xGa_{1-x}As/In_xAl_{1-x}As$ MQW at $T=300$ K in a three-dimensional representation. It is measured by 10 time scans at different wavelengths. The pump spectrum is depicted in Fig. 5.

TABLE II. Summary of the exciton ionization time and the *eh* and/or exciton nonlinearities for different $In_xGa_{1-x}As$ MQW's investigated.

| $L_Z$ (Å) | $\tau$ (fs) | $R_{eh/x}$ |
|---|---|---|
| | $In_xGa_{1-x}As/In_xAl_{1-x}As$ | |
| 100 | 120 | 3.4 |
| 150 | 200 | 2.5 |
| 200 | 200 | 2.7 |
| | $In_xGa_{1-x}As/InP$ | |
| 100 | 100 | 3.9 |

at very low temperatures localization effects play an important role and complicate the interpretation.[20]

In Fig. 11 we finally show (in a three-dimensional representation) the temporal dependence of the differential absorption for the 200-Å $In_xGa_{1-x}As/In_xAl_{1-x}As$ MQW at room temperature, measured for 10 spectral positions around the exciton peak. The central curve is that of Fig. 6. In the spectral interval displayed the cross correlation of the output of the fiber source is constant within 20%, as described in Sec. II. This was determined in an independent measurement.[17] As expected, a maximum at the excitonic position is seen. A detailed analysis of these data reveals that the behavior does not only represent the bleaching of the excitonic line, but also contains a contribution due to broadening of the continuum.

## V. DISCUSSION AND CONCLUSION

We have investigated the femtosecond dynamics of resonantly excited excitons in $In_xGa_{1-x}As$ QW's. As for GaAs QW's, the dynamics is well described by direct creation of excitons that are subsequently dissociated in a few hundred femtoseconds into free *e-h* pairs. Comparison of the measured ionization time $\tau$ with the exciton line broadening by the LO phonon shows that for both materials at room temperature the ionization is mainly due to collisions with LO phonons. Investigation of the temperature dependence of $\tau$, however, reveals that in $In_xGa_{1-x}As$ QW's excitons are also ionized by another process that is weakly temperature dependent and extrinsic. This process contributes to $\approx 1$ meV of the low-temperature exciton linewidth (4 meV). This process cannot be explained by inelastic scattering of excitons with free electrons and holes because it has neither the correct temperature dependence nor the right magnitude. For example, at room temperature and for the typical densities of our experiments, the contribution of this mechanism to the linewidth is estimated to be $\approx 0.1$ meV, corresponding to an ionization time $> 6$ ps.[21] A possible candidate is the ionization of excitons by random fields of ionized impurities with low activation energies and thus a weak temperature dependence.

The other important quantity that we have measured is the ratio between the *e-h* plasma and exciton saturation densities, $R_{eh/x}$. The variation of $R_{eh/x}$ as a function of $E_b$ among different materials ($In_xGa_{1-x}As$ versus GaAs) confirms that occupation of the phase space plays an important role in the optical nonlinearities in QW's. The numerical values obtained by Schmitt-Rink *et al.*[9] seem, however, to overestimate the effects of the *e-h* plasma, thus giving a magnitude of $R_{eh/x}$ somehow smaller than measured. The theory is based on a first-order perturbation expansion of the exciton oscillator strength as a function of the density of excitons or of *e-h* pairs, and accounts for both phase-space filling and exchange interaction. Numerical calculations require summation over the complete set of exciton states, i.e., bound as well as unbound. In Ref. 9 only partial sums were performed. However, recently Zimmermann,[10] using exciton–Green-function techniques, was able to perform exact summations over the whole spectra of exciton states. His numerical solutions give larger values for $R_{eh/x}$. For GaAs at room temperature he gets $R_{eh/x} \approx 2$, in almost perfect agreement with experiment,[7] whereas Schmitt-Rink *et al.* calculated $R_{eh/x} \approx 1$. In the case of $In_xGa_{1-x}As$ QW's Zimmermann's calculation gives $R_{eh/x} = 2$ at 150 K, again in excellent agreement with experiment (see Table I). Unfortunately, explicit numerical results are only given for low values of $k_BT/E_b$, which do not allow a direct comparison at higher temperature. However, extrapolation of his results is also in good agreement with our results ($R_{eh/x} \approx 3$ at $T = 300$ K). The important conclusion of this comparison is that long-range screening does not play an important role at all in the excitonic nonlinearities of QW's which are dominated by the Fermi statistics obeyed by the exciton's constituents.

## ACKNOWLEDGMENTS

We would like to thank Dr. B. Tell for the ion implantation of the samples and Dr. J. H. Kuo for his help in the early phase of this study.

[1]For recent reviews, see the two IEEE J. Quantum Electron. special issues on Quantum Wells and Superlattices [**QE-22**, 1609–1921 (1986), edited by D. S. Chemla and A. Pinczuk and **QE-24**, 1579–1791 (1988), edited by J. Coleman].

[2]D. A. B. Miller, D. S. Chemla, P. W. Smith, A. C. Gossard, and W. Wiegmann, Appl. Phys. B **28**, 96 (1982).

[3]J. S. Weiner, D. S. Chemla, D. A. B. Miller, T. H. Wood, D. Sivco, and A. Y. Cho, Appl. Phys. Lett. **46**, 619 (1985).

[4]H. Temkin, M. B. Panish, P. M. Petroff, R. A. Hamm, J. M. Vandenberg, and S. Sunski, Appl. Phys. Lett. **47**, 394 (1985).

[5]For recent reviews, see D. S. Chemla, D. A. B. Miller, and S. Schmitt-Rink, in *Optical Nonlinearities and Instabilities in Semiconductors*, edited by H. Haug (Academic, New York, 1988); S. Schmitt-Rink, D. S. Chemla, and D. A. B. Miller, Adv. Phys. (to be published).

[6]D. S. Chemla, D. A. B. Miller, P. W. Smith, A. C. Gossard, and W. Wiegmann, IEEE J. Quantum Electron. **QE-20**, 265 (1984).

[7]W. H. Knox, R. L. Fork, M. C. Downer, D. A. B. Miller, D. S. Chemla, C. V. Shank, A. C. Gossard, and W. Wiegmann,

Phys. Rev. Lett. **54**, 1306 (1985).
[8]W. H. Knox, C. Hirlimann, D. A. B. Miller, J. Shah, D. S. Chemla, C. V. Shank, A. C. Gossard, and W. Wiegmann, Phys. Rev. Lett. **56**, 1191 (1986).
[9]S. Schmitt-Rink, D. S. Chemla, and D. A. B. Miller, Phys. Rev. B **32**, 6601 (1985).
[10]R. Zimmermann, Phys. Status Solidi B **146**, 371 (1988).
[11]R. L. Fork, B. I. Greene, and C. V. Shank, Appl. Phys. Lett. **38**, 671 (1981).
[12]W. H. Knox, M. C. Downer, R. L. Fork, and C. V. Shank, Opt. Lett. **9**, 552 (1984).
[13]W. H. Knox, J. Opt. Soc. Am. B **4**, 1771 (1987).
[14]L. F. Mollenauer and R. H. Stolen, Opt. Lett. **9**, 13 (1984).
[15]K. L. Vodop'yanov, A. B. Grudinin, E. M. Dianov, L. A. Kulevskii, A. M. Prokhorov, and D. V. Khaidarov, Sov. J. Quantum Electron. **17**, 1311 (1987).
[16]A. S. Gouveia-Neto, A. S. L. Gomes, and J. R. Taylor, IEEE J. Quantum Electron. **QE-23**, 1938 (1987).
[17]M. N. Islam, G. Sucha, I. Bar-Joseph, M. Wegener, J. P. Jordan, and D. S. Chemla (unpublished).
[18]Z. Vardeny and J. Tauc, Opt. Commun. **39**, 396 (1981).
[19]M. S. Skolnick, K. J. Nash, P. R. Tapster, D. J. Mowbray, S. J. Bass, and A. D. Pitt, Phys. Rev. B **35**, 5925 (1987).
[20]J. Hegarty, K. Tai, and W. T. Tsang, Phys. Rev. B **38**, 7843 (1988).
[21]Y. P. Feng and H. N. Spector, IEEE J. Quantum Electron. **QE-24**, 1659 (1988).